Reduced Graphene Oxide/Copper Nanowire Hybrid Films as High-Performance Transparent Electrodes

Iskandar N. Kholmanov,[†,‡] Sergio H. Domingues,[†,§] Harry Chou,[†] Xiaohan Wang,[†] Cheng Tan,[†] Jin-Young Kim,[†] Huifeng Li,[†] Richard Piner,[†] Aldo J. G. Zarbin,[§] and Rodney S. Ruoff[†,*]

[†]Department of Mechanical Engineering and the Materials Science and Engineering Program, The University of Texas at Austin, 1 University Station C2200, Austin, Texas 78712, United States, [‡]CNR-IDASC Sensor Lab Department of Chemistry and Physics, University of Brescia, via Valotti, 9, Brescia 25133, Italy, and [§]Department of Chemistry, Universidade Federal do Paranà, CP 19081, CEP 81531-990, Curitiba, PR, Brazil

ABSTRACT Hybrid films composed of reduced graphene oxide (RG-O) and Cu nanowires (NWs) were prepared. Compared to Cu NW films, the RG-O/Cu NW hybrid films have improved electrical conductivity, oxidation resistance, substrate adhesion, and stability in harsh environments. The RG-O/Cu NW films were used as transparent electrodes in Prussian blue (PB)-based electrochromic devices where they performed significantly better than pure Cu NW films.

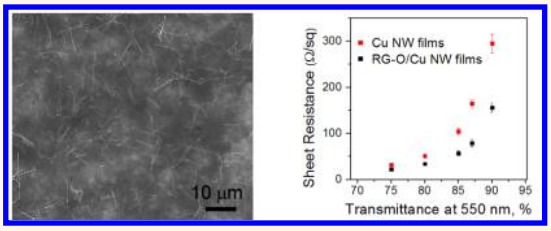

KEYWORDS: reduced graphene oxide · copper nanowires · hybrid films · transparent conductive films

Electrical and optical properties of metal nanowire (NW) films make them promising materials for transparent conductive film (TCF) applications. It has been demonstrated that Au NW,[1,2] Ag NW,[3,4] and Cu NW films[5−7] can have sheet resistances (R_s) comparable to or lower than commonly used indium tin oxide (ITO) films at the same optical transmittance (T). Metal NW films on plastic substrates can have better mechanical properties than ITO films for flexible electronics.[4−6] However, metal NW films can have low oxidation resistance, poor adhesion to the substrate, and low stability in harsh environments. NW films have electrically nonconductive open spaces, while some applications require continuously conductive regions. One strategy to overcome the drawbacks of metal NW films involves the addition of components such as metal nanoparticles, thin metal films, oxide nanostructures, or conductive polymers.[8−12] Typically, the added constituent can only address one of the weaknesses of NW films, and adding multiple constituents may lead to processing and cost-related issues.

In this context, reduced graphene oxide (RG-O) offers versatile functional properties.[13−17] We recently demonstrated[18] that the addition of RG-O into metal NW films resulted in hybrid films with improved electrical conductivity, as RG-O provides two-dimensional pathways for charge transfer between nonpercolated metal NWs. Here, we show that RG-O platelets deposited on top of Cu NW films simultaneously address multiple problems, acting as an oxidation-resistant layer, a conductive and continuous transparent film that fills in open spaces between NWs, and an additional material that protects the NWs from harsh environments.

RESULTS AND DISCUSSION

Cu NWs (average length >20 μm, average diameter <60 nm, purchased from NanoForge) were dispersed in a mixture of 97.0 vol % isopropyl alcohol (IPA) and 3.0 vol % hydrazine monohydrate ($N_2H_4 \cdot H_2O$) at a concentration of ~1.2 mg/mL. Spray coating of this dispersion onto a target substrate yields a thin film of randomly oriented Cu NWs with open spaces between them (Figure 1a). RG-O films were fabricated by spin coating a dispersion of graphene oxide (G-O) platelets, followed by chemical and thermal reduction processes (see Methods). The resulting RG-O films have a continuous and smooth surface morphology, as shown by atomic force microscopy (AFM) in Figure 1b.

* Address correspondence to r.ruoff@mail.utexas.edu.

Received for review December 28, 2012 and accepted January 28, 2013.

Published online January 29, 2013
10.1021/nn3060175

© 2013 American Chemical Society

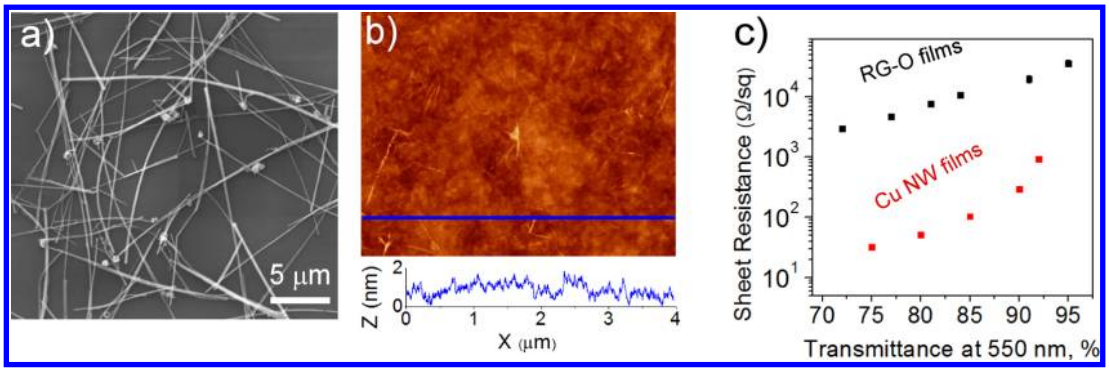

Figure 1. (a) SEM image of a network of Cu NWs on a SiO_2/Si substrate. (b) AFM image of RG-O films on a SiO_2/Si substrate. The line profile shows a smooth surface. (c) Optical transmittance and sheet resistance of spin-coated RG-O and spray-coated Cu NW films.

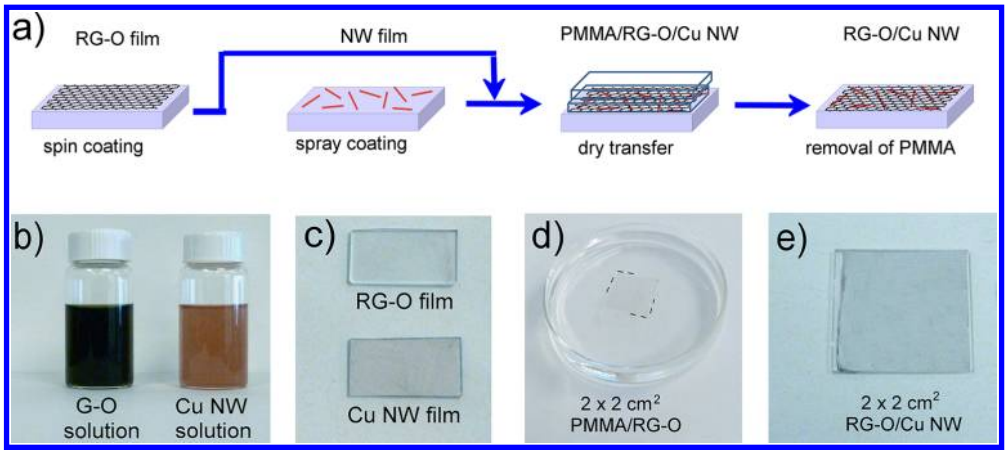

Figure 2. (a) Schematic of preparation of RG-O/Cu NW hybrid films. (b) Photographs of G-O dispersed in water (1.0 mg/mL) and Cu NWs dispersed in IPA with 3.0 vol % $N_2H_4 \cdot H_2O$ (1.2 mg/mL). (c) RG-O (top) and Cu NW (bottom) films on glass substrates. (d) A 2 × 2 cm^2 PMMA/RG-O film delaminated from the glass substrate in 1 M aqueous solution of NaOH. (e) Photograph of 2 × 2 cm^2 RG-O/Cu NW films on a glass substrate after the PMMA layer was removed.

The sheet resistance and optical transmittance of the Cu NW and RG-O films are listed in Figure 1c. To improve electrical conductivity, the as-deposited Cu NW films were annealed in a tube furnace at 180 °C for 30 min under Ar (95%) + H_2 (5%) at 1 atm pressure. The Cu NW films with an optical transmittance at 550 nm of $T_{550} > 95\%$ had no globally connected network of NWs (*i.e.*, the films were nonconductive). Longer spraying time increases the density of NWs, yielding percolated networks, and decreases both the T_{550} and R_s of the films. Typical films with $T_{550} = 90\%$ have a sheet resistance of $R_s = 295 \pm 19.5$ Ω/sq. Typical RG-O films with $T_{550} = 90\%$ have a sheet resistance of $R_s = 19.6 \pm 2.7$ kΩ/sq. Contributing to the R_s of the RG-O films are structural defects and junction resistances between RG-O platelets.[18]

Figure 2a shows a schematic detailing the assembly process of RG-O films onto Cu NW films. The dispersions of the Cu NWs (1.2 mg/mL) and G-O (1.0 mg/mL) shown in Figure 2b were used to produce thin films (Figure 2c) of Cu NWs and RG-O by spray and spin coating, respectively. A poly(methyl methacrylate) (PMMA) was spin coated on top of the RG-O films, and the resulting PMMA/RG-O film was subsequently delaminated from the glass substrate in 1 M NaOH aqueous solution (Figure 2d), as described elsewhere.[19] The delaminated PMMA/RG-O films were washed several times with deionized (DI) water in order to remove the residual NaOH and then transferred on top of Cu NW films using a dry transfer method.[20,21] After transfer, the PMMA layer was removed with acetone, resulting in the final RG-O/Cu NW hybrid films as shown in Figure 2e. To improve electrical conductivity, the obtained RG-O/Cu NW films were annealed in a tube furnace at 180 °C for 30 min under a Ar (95%) + H_2 (5%) gas mixture at 1 atm pressure.

Figure 3a shows sheet resistances and optical transmittances of the composite films. The RG-O films used in the hybrid film fabrication had $R_s = 36.6 \pm 4.7$ kΩ/sq and $T_{550} = 95.5\%$. The hybrid films had $R_s = 34 \pm 2.6$ Ω/sq at $T_{550} = 80\%$, which can be compared to pure Cu NW films ($R_s = 51 \pm 4.0$ Ω/sq) and pure RG-O films ($R_s = 7.6 \pm 0.86$ kΩ/sq), each also at $T_{550} = 80\%$. Individual Cu NWs with an average length >20 μm can connect two or more RG-O platelets, and the metallic conductivity of these NWs can decrease or eliminate the platelet–platelet junction resistance.[18] In turn, the film of overlapped and stacked RG-O platelets can bridge initially

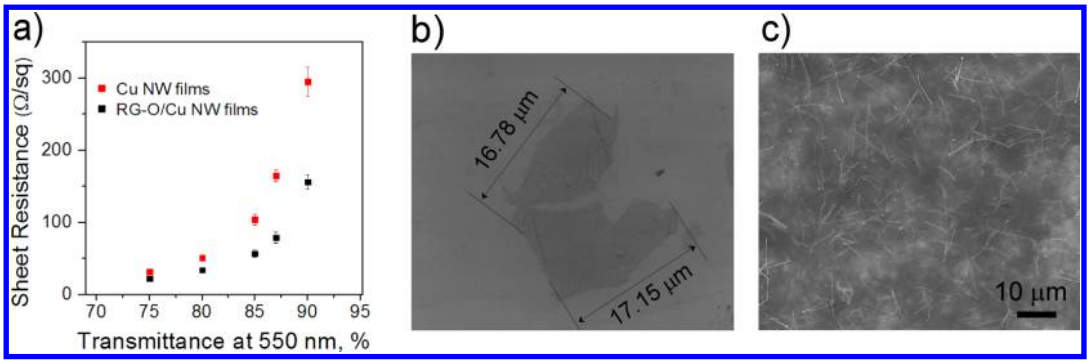

Figure 3. (a) Transmittance and sheet resistance of the pure Cu NW films and RG-O/Cu NW hybrid films. (b) SEM image of individual RG-O platelets with lateral sizes indicated. (c) SEM image of a typical RG-O/Cu NW film.

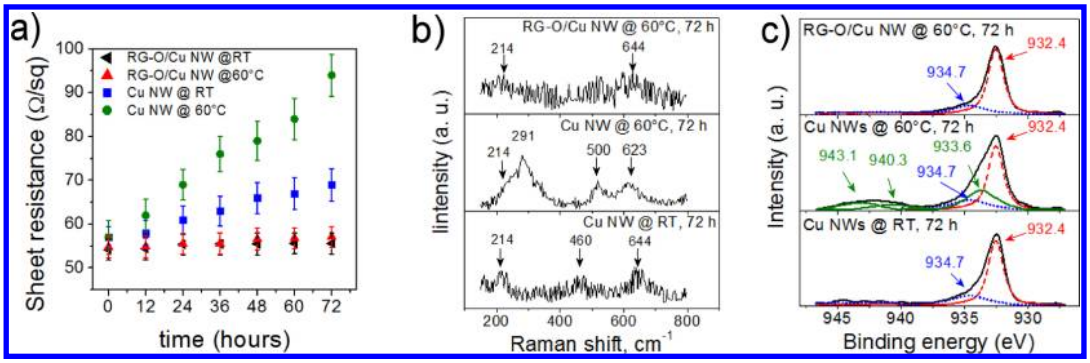

Figure 4. (a) Changes in R_s of pure Cu NW films and RG-O/Cu NW hybrid films kept at room temperature (RT) and also at 60 °C, each for 72 h. (b) Raman spectra of Cu NW films kept at room temperature (bottom) and 60 °C (middle) for 72 h and of RG-O/Cu NW films kept at 60 °C for 72 h (top). (c) Cu $2p_{3/2}$ XPS spectrum of Cu NW film kept at room temperature (bottom) and 60 °C (middle) for 72 h, and of RG-O/Cu NW films kept at 60 °C for 72 h (top).

nonconnected Cu NWs. The lateral size of RG-O platelets may be as large as several micrometers, as shown in Figure 3b. A single RG-O platelet with such a lateral size can bridge two or more nonconnected Cu NWs separated by any distance smaller than the lateral size of the platelet. This may result in higher electrical conductivity of the hybrid films because of the absence of RG-O interplatelet junction resistances. Without RG-O platelets, the nonconnected Cu NWs cannot contribute to the electrical conductivity of the Cu NW films. The continuous RG-O film also eliminates the empty spaces between NWs, as shown in Figure 3c, and provides a two-dimensional conductive platform for charge carriers, which is particularly attractive for dye-sensitized solar cells.[22] Overall, the synergy between Cu NWs and RG-O platelets allows for the fabrication of hybrid films with electrical conductivity better than pure RG-O and pure Cu NW films.

The RG-O film can also protect the Cu NWs underneath it from oxidation, resulting in improved stability of the hybrid film. Figure 4a shows the change of R_s over time of pure Cu NW and hybrid RG-O/Cu NW films in ambient atmosphere at room temperature and at 60 °C. The room temperature R_s of Cu NW films increases from 57 ± 2.5 Ω/sq (as-prepared sample) to 69 ± 3.2 Ω/sq after 72 h, and the R_s of the samples at 60 °C increases from 56 ± 2.5 Ω/sq (as-prepared sample) to 94 ± 4.7 Ω/sq also after 72 h. The change in R_s values is due to the oxidation of the Cu NW films, and the more rapid increase at 60 °C is due to the faster kinetics of oxidation at higher temperatures.[10] The R_s of the hybrid RG-O/Cu NW films shows no significant change after 72 h at room temperature and also at 60 °C. This is consistent with Raman spectroscopy studies (Figure 4b). Cu NW films, kept at room temperature for 72 h, show Raman peaks at about 214, 460, and 644 cm^{-1}. The Raman spectrum of the Cu NW films kept at 60 °C for 72 h exhibits the same peaks but with higher intensity and several additional peaks in the range of 200−800 cm^{-1}. These Raman peaks are due to different copper oxides: CuO (299, 342, 500, 634 cm^{-1}), Cu_2O (214, 644 cm^{-1}), $Cu(OH)_2$ (450−470 cm^{-1}, 540−580 cm^{-1}).[23−25] The higher intensity Raman peaks of the Cu NW films held at 60 °C for 72 h, compared to the room temperature sample, along with the presence of CuO peaks, indicate a higher oxidation level (*i.e.*, likely a thicker oxide layer) of the Cu NWs. In contrast, Raman spectra of RG-O/Cu NW hybrid films show only low-intensity peaks at around 214 and 644 cm^{-1} due to the surface Cu_2O layer formed during the film fabrication processes. The spectra of the hybrid films (72 h at room temperature or at 60 °C) are similar to that of the pure Cu NW films directly after fabrication (see Supporting Information).

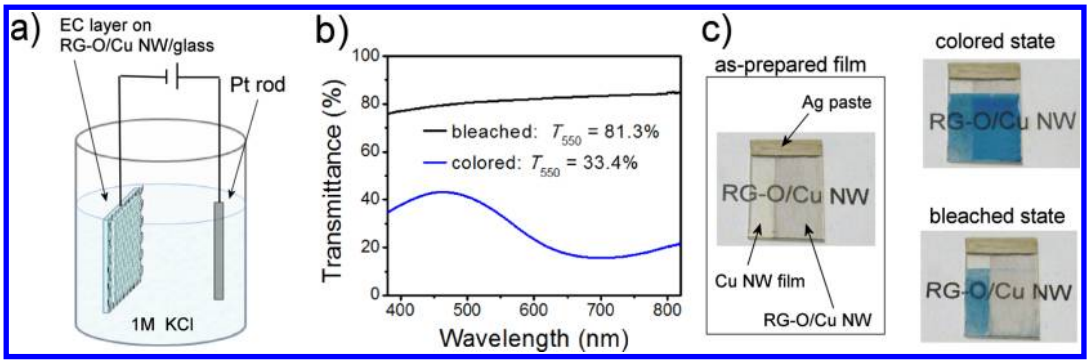

Figure 5. (a) Schematic of an electrochromic device in an electrolyte solution. (b) Optical transmittance spectra of colored and bleached states of PB films deposited on a RG-O/Cu NW transparent electrode. (c) As-prepared mixed transparent electrode composed of pure Cu NW films (left) and RG-O/Cu NW films (right). Initial (colored) state (right top) and bleached state (right bottom) of PB deposited on the mixed electrode.

X-ray photoelectron spectroscopy (XPS) studies of these films (Figure 4c) at binding energies of Cu $2p_{3/2}$ (932.4 eV) were done to further evaluate the possible protection against oxidation by the RG-O film. The bottom spectrum in Figure 4c was obtained from pure Cu NW films held at room temperature for 72 h. The high-intensity peak (dashed red curve) at ~932.4 eV is assigned to the spectral overlap of Cu $2p_{3/2}$ and Cu_2O,[26] and the low-intensity peak (dotted blue curve) at ~934.7 eV is assigned to $Cu(OH)_2$.[27] The spectrum obtained from the Cu NW film held at 60 °C for 72 h shows a peak that can be deconvoluted into peaks that correspond to $Cu(OH)_2$ (934.7 eV) (dotted blue curve), CuO (933.6 eV), and the shakeup satellites of CuO (940.3 and 943.1 eV) (solid dark green curves).[26,28] The presence of different copper oxides in the latter spectrum indicates the higher level of oxidation of the Cu NW film held at 60 °C for 72 h. These copper oxide compounds were not observed in the XPS spectra of RG-O/Cu NW films, which are similar to that of the as-prepared Cu NW films (see Supporting Information). These data show the high stability of the RG-O/Cu NW films against oxidation, and that the RG-O layer protects the underlying Cu NWs from oxidation.

Recent reports show the improved electrical conductivity of hybrid films composed of Cu metal grids[29] and Cu NWs[30] assembled with graphene grown by chemical vapor deposition (CVD). In contrast, our results on RG-O/Cu NW hybrid films provide a solution-based route to fabricate both the single-component and hybrid films. Additionally, compared to RG-O/Ag NW hybrid films reported in our prevous work,[18] RG-O/Cu NW films are more cost-effective as Cu NWs that are significantly less expensive than Ag NWs.[6] In addition, our results on oxidation resistance of RG-O/Cu NW hybrid films are consistent with the recent studies on the protection of metal surfaces from oxidation with RG-O films[17] and CVD-graphene grown onto metal substrates.[24] Another approach to improve the oxidation resistance of Cu NW films is by coating Cu NWs with a Ni shell that yields oxidation-resistant cupronickel NWs.[10] However, compared to RG-O, the Ni coating addresses only the oxidation of Cu NWs and lowers the aspect ratio of the Cu NWs, which can adversely affect the optical transmittance of the films.[31]

The RG-O/Cu NW hybrid films were tested as a transparent electrode in Prussian blue (PB)-based electrochromic (EC) devices. Typical PB-based EC devices are composed of a PB layer deposited onto an ITO transparent electrode. Electrochemical reactions, induced by an applied external electric field, cause reversible modulations in the optical properties of PB layers. Color changes from blue to colorless upon reduction are caused by the conversion of a mixed-valence (Fe^{2+}, Fe^{3+}) compound into a single-valence (Fe^{2+}) compound (and *vice versa* upon oxidation) that can be described as[32,33]

$$\text{(blue)}Fe_4^{3+}[Fe^{2+}(CN)_6]_3 + 4K^+ + 4e^- \leftrightarrow \text{(colorless)}K_4Fe_4^{2+}[Fe^{2+}(CN)_6]_3$$

In our studies, ITO electrodes were replaced by RG-O/Cu NW electrodes on glass substrates. EC PB layers on top of the RG-O/Cu NW transparent electrodes have been electrochemically deposited using an aqueous solution of 0.05 M hyrdochloric acid (HCl), 0.05 M potassium hexacyanoferrate (III) ($K_3[Fe(CN)_6]$), and 0.05 M iron(III) chloride ($FeCl_3$) in a 1:2:2 ratio.[34,35] Applying an external field between the RG-O/Cu NW electrode and a Pt counter electrode, both immersed into the solution, results in the homogeneous deposition of PB layers onto the RG-O/Cu NW electrode (see Supporting Information).[33,34]

Optical property modulation of the deposited PB layers by the redox process has been tested using 1 M KCl aqueous solution as an electrolyte (Figure 5a). Electrochemical reduction of PB induced by an external voltage (−0.6 V to the RG-O/Cu NW TCF) yields colorless EC layers. Application of a reverse external field induces an oxidation process, which generates mixed-valence compounds and yields a blue color of the EC layers. The optical transmittance corresponding to the bleached (T_{550} = 79.2%) and colored (T_{550} = 36.4%)

states of the PB are shown in Figure 5b. Typical coloration and bleaching times for 90% transmittance change are 75 and 95 s, respectively. These values are close to that of an EC device using the same PB EC film and same electrolyte but with an ITO electrode.[32−34]

Such PB EC films with reversible coloration/bleaching properties cannot be obtained using pure Cu NW transparent electrodes; indeed, a mixed transparent electrode (a glass substrate with one-half covered by pure Cu NW film and the other by RG-O/Cu NW hybrid film, Figure 5c, as-prepared film) was made that shows this. Homogeneous PB layers were deposited on top of the electrode (Figure 5c, colored state). In electrochemical bleaching processes, the PB layers on top of the RG-O/Cu NW film have been completely bleached, while no bleaching of the PB layer deposited on the pure Cu NW film was observed (Figure 5c, bleached state). This is because pure Cu NWs form copper hexacyanoferrate compounds during the deposition of PB layers.[36−38] During the process of formation of these compounds, the Cu NW networks have been destroyed, and consequently, this electrode lost its high electrical conductivity. Also, Cu NW films immersed into the electrolyte solution partially delaminate from the substrate, which also leads to the loss of NW network conductivity. In contrast, in RG-O/Cu NW films, the RG-O layer protects the Cu NWs from reacting with the harsh solution used for PB deposition, which allows for repeatable cycling and homogeneous optical modulation of the PB EC layer, and there was no delamination of the RG-O/Cu NW hybrid films when immersed in the KCl solution.

CONCLUSION

A film composed of RG-O platelets assembled onto a Cu NW film layer yields hybrid films with improved electrical conductivity, 2-D film continuity (no empty regions such as gaps between NWs), higher oxidation resistance, and better adhesion to the substrate than pure Cu NW films. EC device performance demonstrates that RG-O, acting as a protective layer for Cu NWs in harsh environments, makes these types of hybrid TCFs suitable for a wider range of applications than pure metal NW films.

METHODS

Fabrication of Cu NW Films. Cu NWs with a concentration of 1 mg/mL in aqueous solution containing 1% diethylhydroxylamine (DEHA) to prevent oxidation and 1% polyvinylpyrrolidone (PVP) to prevent aggregation were purchased from NanoForge. Cu NWs were separated from the solution by centrifugation (2000 rpm for 5 min). After the supernatant was removed, the NW sediment was redispersed in isopropyl alcohol (IPA) mixed with 3.0 vol % hydrazine monohydrate ($N_2H_4 \cdot H_2O$) to prevent oxidation of Cu NWs by vortexing for 3−4 min. This process was repeated four times in order to remove the PVP from the NW suspension. A 1.2 mg/mL dispersion of Cu NWs in IPA (having well-dispersed Cu NWs, Figure 1) was used for spray coating. Higher (>1.2 mg/mL) concentrations of Cu NWs in the dispersion resulted in agglomerated NWs, and when spray-coated, these adversely affect Cu NW film optical properties. Repeated spray coating yields the desired density of Cu NWs on the substrate. Between each sprayed pulse, complete drying of the sprayed droplets on the substrate was obtained. Keeping the substrate at about 60 °C and delicately blowing it with nitrogen gas accelerated the drying process.

Fabrication of RG-O Films. Graphite oxide was produced from natural graphite (SP-1, Bay Carbon) using a modified Hummers method, as described elsewhere.[39] Aqueous dispersions of G-O at various concentrations were prepared by stirring graphite oxide solids in pure water (18.0 MΩ·cm resistivity, purchased from Barnstead) for 3 h, and then sonicating the resulting mixture (VWR B2500A-MT bath sonicator) for 45 min. The G-O dispersions were then spin-coated onto glass substrates using a spin speed of 4000 rpm for 2 min. The obtained G-O films were subsequently reduced using hydrazine monohydrate ($N_2H_4 \cdot H_2O$) vapor for 24 h, keeping the samples at 90 °C,[18] and were then thermally annealed at 400 °C for 1 h in an Ar (95%) + H (5%) gas mixture at 1 atm pressure. RG-O films, obtained by spin coating of an aqueous G-O dispersion with a concentration of 1.0 mg/mL, possess $R_s = 36.6 \pm 4.7$ kΩ/sq, $T_{550} = 95.5\%$, and an average thickness of about 0.8 nm. The latter films were used to fabricate RG-O/Cu NW hybrid films.

Characterization of Films. SEM (Hitachi S-5500 SEM equipped with STEM) and AFM (Park Systems Model XE-100 AFM) were used to characterize the structural properties of the nanostructures and thin films. Optical transmittances (T) were measured using ultraviolet−visible−near-infrared (UV−vis−NIR) spectroscopy (Cary 5000) and spectroscopic ellipsometry (J.A. Wollam M2000). R_s was measured with the four-probe van der Pauw method: four gold electrodes were deposited on the film in a square configuration with dimensions of ~6 × 6 mm^2. Raman spectroscopy (WITEC Alpha300, $\lambda = 488$ nm, 100× objective) measurements were carried out to study the oxidation of Cu NWs. XPS experiments were performed on a Kratos photoelectron spectroscopy system equipped with an Al Kα monochromator X-ray source operating at a power of 350 W. Binding energies were determined relative to the metallic copper Cu $2p_{3/2}$ binding energy of 932.4 eV. Deconvolution of XPS spectra were obtained resolved by fitting each peak with a combined Guassian−Lorentzian function after background subtraction.

Conflict of Interest: The authors declare no competing financial interest.

Acknowledgment. This work was supported by a Tokyo Electron Ltd. (TEL)-customized Semiconductor Research Corporation award (Project #2009-OJ-1873_development of graphene-based transparent conductive films for display applications). We thank D. Toma, J. Li, and J. Faguet for discussion and comments. A.J.G.Z. and S.H.D. gratefully acknowledge the CNPq, INCT of Carbon Nanomaterials (CNPq), NENNAM (Pronex F. Araucária/CNPq), and CAPES and CNPq for the scholarship.

Supporting Information Available: Synthesis and characterization of RG-O/Cu NW hybrid films; additional information on Raman spectra and XPS data; and some details of electrochromic devices are presented. This material is available free of charge *via* the Internet at http://pubs.acs.org.

REFERENCES AND NOTES

1. Lyons, P. E.; De, S.; Elias, J.; Schamel, M.; Philippe, L.; Bellew, A. T.; Boland, J. J.; Coleman, J. N. High-Performance Transparent Conductors from Networks of Gold Nanowires. *J. Phys. Chem. Lett.* **2011**, *2*, 3058–3062.
2. Azulai, D.; Belenkova, T.; Gilon, H.; Barkay, Z.; Markovich, G. Transparent Metal Nanowire Thin Films Prepared in

Mesostructured Templates. *Nano Lett.* **2009**, *9*, 4246–4249.
3. Leem, D. S.; Edwards, A.; Faist, M.; Nelson, J.; Bradley, D. D. C.; de Mello, J. C. Efficient Organic Solar Cells with Solution-Processed Silver Nanowire Electrodes. *Adv. Mater.* **2011**, *23*, 4371–4375.
4. Lee, J. Y.; Connor, S. T.; Cui, Y.; Peumans, P. Solution-Processed Metal Nanowire Mesh Transparent Electrodes. *Nano Lett.* **2008**, *8*, 689–692.
5. Wu, H.; Hu, L.; Rowell, M. W.; Kong, D.; Cha, J. J.; McDonough, J. R.; Zhu, J.; Yang, Y.; McGehee, M. D.; Cui, Y. Electrospun Metal Nanofiber Webs as High-Performance Transparent Electrode. *Nano Lett.* **2010**, *10*, 4242–4248.
6. Rathmell, A. R.; Wiley, B. J. The Synthesis and Coating of Long, Thin Copper Nanowires To Make Flexible, Transparent Conducting Films on Plastic Substrates. *Adv. Mater.* **2011**, *23*, 4798–4803.
7. Zhang, D.; Wang, R.; Wen, M.; Weng, D.; Cui, X.; Sun, J.; Li, H.; Lu, Y. Synthesis of Ultralong Copper Nanowires for High-Performance Transparent Electrodes. *J. Am. Chem. Soc.* **2012**, *134*, 14283–14286.
8. Hu, L.; Kim, H. S.; Lee, J. Y.; Peumans, P.; Cui, Y. Scalable Coating and Properties of Transparent, Flexible, Silver Nanowire Electrodes. *ACS Nano* **2010**, *4*, 2955–2963.
9. Morgenstern, F. S. F.; Kabra, D.; Massip, S.; Brenner, T. J. K.; Lyons, P. E.; Coleman, J. N.; Friend, R. H. Ag-Nanowire Films Coated with ZnO Nanoparticles as a Transparent Electrode for Solar Cells. *Appl. Phys. Lett.* **2011**, *99*, 183307.
10. Rathmell, A. R.; Nguyen, M.; Chi, M.; Wiley, B. J. Synthesis of Oxidation-Resistant Cupronickel Nanowires for Transparent Conducting Nanowire Networks. *Nano Lett.* **2012**, *12*, 3193–3199.
11. Zhu, R.; Chung, C.-H.; Cha, K. C.; Yang, W.; Zheng, Y. B.; Zhou, H.; Song, T.-B.; Chen, C.-C.; Weiss, P. S.; Li, G.; *et al.* Fused Silver Nanowires with Metal Oxide Nanoparticles and Organic Polymers for Highly Transparent Conductors. *ACS Nano* **2011**, *5*, 9877–9882.
12. Gaynor, W.; Burkhard, G. F.; McGehee, M. D.; Peumans, P. Smooth Nanowire/Polymer Composite Transparent Electrodes. *Adv. Mater.* **2011**, *23*, 2905–2910.
13. Park, S.; Ruoff, R. S. Chemical Methods for the Production of Graphenes. *Nat. Nanotechnol.* **2009**, *4*, 217–224.
14. Wu, J. B.; Agrawal, M.; Becerril, H. A.; Bao, Z. N.; Liu, Z. F.; Chen, Y. S.; Peumans, P. Organic Light-Emitting Diodes on Solution-Processed Graphene Transparent Electrodes. *ACS Nano* **2010**, *4*, 43–48.
15. Becerril, H. A.; Mao, J.; Liu, Z.; Stoltenberg, R. M.; Bao, Z.; Chen, Y. Evaluation of Solution-Processed Reduced Graphene Oxide Films as Transparent Conductors. *ACS Nano* **2008**, *2*, 463–470.
16. Eda, G.; Chhowalla, M. Chemically Derived Graphene Oxide: Towards Large-Area Thin-Film Electronics and Optoelectronics. *Adv. Mater.* **2010**, *22*, 2392–2415.
17. Kang, D.; Kwon, J. Y.; Cho, H.; Sim, J.-H.; Hwang, H. S.; Kim, C. S.; Kim, Y. J.; Ruoff, R. S.; Shin, H. S. Oxidation Resistance of Iron and Copper Foils Coated with Reduced Graphene Oxide Multilayers. *ACS Nano* **2012**, *6*, 7763–7769.
18. Kholmanov, I. N.; Stoller, M.; Edgeworth, J.; Lee, W. H.; Li, H.; Lee, J.; Barnhart, C.; Potts, J.; Piner, R.; Akinwande, D.; *et al.* Nanostructured Hybrid Transparent Conductive Films with Antibacterial Properties. *ACS Nano* **2012**, *6*, 5157–5163.
19. Yamaguchi, H.; Eda, G.; Mattevi, C.; Kim, H. K.; Chhowalla, M. Highly Uniform 300 mm Wafer-Scale Deposition of Single and Multilayered Chemically Derived Graphene Thin Films. *ACS Nano* **2010**, *4*, 524–528.
20. Suk, J. W.; Kitt, A.; Magnuson, C. W.; Hao, Y.; Ahmed, S.; An, J.; Swan, A. K.; Goldberg, B. B.; Ruoff, R. S. Transfer of CVD-Grown Monolayer Graphene onto Arbitrary Substrates. *ACS Nano* **2011**, *5*, 6916–6924.
21. Kholmanov, I. N.; Magnuson, C. W.; Aliev, A. E.; Li, H.; Zhang, B.; Suk, J. W.; Zhang, L. L.; Peng, E.; Mousavi, S. H.; Khanikaev, A. B.; *et al.* Improved Electrical Conductivity of Graphene Films Integrated with Metal Nanowires. *Nano Lett.* **2012**, *12*, 5679–5683.
22. Yen, M.-Y.; Hsiao, M.-C.; Liao, S.-H.; Liu, P.-I.; Tsai, H.-M.; Ma, C.-C. M.; Pu, N.-W.; Ger, M.-D. Preparation of Graphene/Multi-Walled Carbon Nanotubes Hybrid and Its Use as Photoanodes of Dye-Sensitized Solar Cells. *Carbon* **2011**, *49*, 3597–3606.
23. Chou, M. H.; Liu, S. B.; Huang, C. Y.; Wu, S. Y.; Cheng, C. L. Confocal Raman Spectroscopic Mapping Studies on a Single CuO Nanowire. *Appl. Surf. Sci.* **2008**, *254*, 7539–7543.
24. Chen, S.; Brown, L.; Levendorf, M.; Cai, W.; Ju, S.-Y.; Edgeworth, J.; Li, X.; Magnuson, C. W.; Velamakanni, A.; Piner, R. D.; *et al.* Oxidation Resistance of Graphene-Coated Cu and Cu/Ni Alloy. *ACS Nano* **2011**, *5*, 1321–1327.
25. Niaura, G. Surface-Enhanced Raman Spectroscopic Observation of Two Kinds of Adsorbed OH-Ions at Copper Electrode. *Electrochim. Acta* **2000**, *45*, 3507–3519.
26. Wu, C.-K.; Yin, M.; O'Brien, S.; Koberstein, J. T. Quantitative Analysis of Copper Oxide Nanoparticle Composition and Structure by X-ray Photoelectron Spectroscopy. *Chem. Mater.* **2006**, *18*, 6054–6058.
27. Dubè, E. C.; Workie, B.; Kounaves, S. P.; Robbat, A., Jr.; Aksu, M. L.; Davies, G. Electrodeposition of Metal Alloy and Mixed Oxide Films Using a Single-Precursor Tetranuclear Copper−Nickel Complex. *J. Electrochem. Soc.* **1995**, *142*, 3357–3365.
28. Poulston, S.; Parlett, P. M.; Stone, P.; Bowker, M. Surface Oxidation and Reduction of CuO and Cu_2O Studied Using XPS and XAES. *Surf. Interface Anal.* **1996**, *24*, 311–320.
29. Zhu, Y.; Sun, Z.; Yan, Z.; Jin, Z.; Tour, J. M. Rational Design of Hybrid Graphene Films for High-Performance Transparent Electrodes. *ACS Nano* **2011**, *5*, 6472–6479.
30. Liang, J.; Bi, H.; Wan, D.; Huang, F. Novel Cu Nanowires/Graphene as the Back Contact for CdTe Solar Cells. *Adv. Funct. Mater.* **2012**, *22*, 1267–1271.
31. Sorel, S.; Lyons, P. E.; De, S.; Dickerson, J. C.; Coleman, J. N. The Dependence of the Optoelectrical Properties of Silver Nanowire Networks on Nanowire Length and Diameter. *Nanotechnology* **2012**, *23*, 185201.
32. Lundgren, C. A.; Murray, R. W. Observations on the Composition of Prussian Blue Films and Their Electrochemistry. *Inorg. Chem.* **1988**, *27*, 933–939.
33. Karyakin, A. A. Prussian Blue and Its Analogues: Electrochemistry and Analytical Applications. *Electroanalysis* **2001**, *13*, 813–819.
34. Lupu, S.; Mihailciuc, C.; Pigani, L.; Seeber, R.; Totir, N.; Zanardi, C. Electrochemical Preparation and Characterisation of Bilayer Films Composed by Prussian Blue and Conducting Polymer. *Electrochem. Commun.* **2002**, *4*, 753–758.
35. Nossol, E.; Zarbin, A. J. G. Electrochromic Properties of Carbon Nanotubes/Prussian Blue Nanocomposite Films. *Sol. Energy Mater. Sol. Cells* **2013**, *109*, 40–46.
36. Chen, S. M.; Chan, C. M. Preparation, Characterization, and Electrocatalytic Properties of Copper Hexacyanoferrate Film and Bilayer Film Modified Electrodes. *J. Electroanal. Chem.* **2003**, *543*, 161–173.
37. Makowski, O.; Stroka, J.; Kulesza, P. J.; Malik, M. A.; Zbigniew, G. Electrochemical Identity of Copper Hexacyanoferrate in the Solid-State: Evidence for the Presence and Redox Activity of Both Iron and Copper Ionic Sites. *J. Electroanal. Chem.* **2002**, *532*, 157–164.
38. Adekola, F.; Fedoroff, M.; Ayrault, S.; Loos-Neskovic, C.; Garnier, E.; Yu, L. T. Interaction of Silver Ions in Solution with Copper Hexacyanoferrate (II) $Cu_2Fe(CN)_6$. *J. Solid State Chem.* **1997**, *132*, 399–406.
39. Stankovich, S.; Dikin, D. A.; Dommett, G. H. B.; Kohlhaas, K. M.; Zimney, E. J.; Stach, E. A.; Piner, R. D.; Nguyen, S. B. T.; Ruoff, R. S. Graphene-Based Composite Materials. *Nature* **2006**, *442*, 282–286.